

Exciton-polaritons in multilayer WSe₂ in a planar microcavity

M. Król,¹ K. Rehcńska,¹ K. Nogajewski,¹ M. Grzeszczyk,¹ K. Łempicka,¹ R. Mirek,¹ S. Piotrowska,¹ K. Watanabe,² T. Taniguchi,² M. R. Molas,¹ M. Potemski,^{1,3} J. Szczytko,¹ and B. Piętka^{1,*}

¹*Institute of Experimental Physics, Faculty of Physics,
University of Warsaw, ul. Pasteura 5, PL-02-093 Warsaw, Poland*

²*National Institute for Materials Science, Tsukuba, Ibaraki, 305-0044, Japan*

³*Laboratoire National des Champs Magnétiques Intenses,
CNRS-UGA-UPS-INSA-EMFL, Grenoble, France*

Due to high binding energy and oscillator strength, excitons in thin flakes of transition metal dichalcogenides constitute a perfect foundation for realizing a strongly coupled light-matter system. In this paper we investigate mono- and few-layer WSe₂ flakes encapsulated in hexagonal boron nitride and incorporated into a planar dielectric cavity. We use an open cavity design which provides tunability of the cavity mode energy by as much as 150 meV. We observe a strong coupling regime between the cavity photons and the neutral excitons in direct-bandgap monolayer WSe₂, as well as in few-layer WSe₂ flakes exhibiting indirect bandgap. We discuss the dependence of the exciton's oscillator strength and resonance linewidth on the number of layers and predict the exciton-photon coupling strength.

I. INTRODUCTION

The possibility to engineer multilayered structures using two-dimensional (2D) van der Waals materials allows to construct new artificial crystals of designed functionalities [1] with strong application potential in photonics and opto-electronics [2], including, especially, the areas of photo-detectors, ultrathin-film photovoltaic devices, light emitting diodes and lasers [3–7].

Optical properties of monolayer (ML) transition metal dichalcogenides (TMDs) are widely explored as they are dominated by particularly strong exciton resonances stable up to room temperatures [8, 9]. This is a consequence of their direct bandgap in contrast to few-layer and bulk forms that exhibit indirect optical transitions [10–12]. These properties make ML TMDs interesting for laser light sources [13–15] and light-matter interactions which demand narrow-resonance oscillators [16, 17]. For ML, the lowest energy transition occurs between the band-edge states at the K^\pm points of the Brillouin zone, which are mostly composed of the transition metal atom orbitals: $d_{x^2-y^2} \pm id_{xy}$ orbitals in the valence band (VB) and d_{z^2} orbitals in the conduction band (CB). Starting from the bilayer, an indirect transition between the band-edge states at the Γ point in the VB and the Q point in the CB appears, as those states are partially composed of p_z orbitals of the chalcogen atoms, which significantly overlap between the layers [18–20].

For a long time the indirect bandgap of multilayer TMDs was considered a drawback in the construction of opto-electronic devices due to low emission rate and poor quantum efficiency. However, compared to the ML, multilayers of TMDs have also several advantages as they possess larger optical density of states and exhibit higher absorbance as well as longer exciton lifetimes [21]. It is

also possible to tune the bandgap and alter the carrier type in TMD-based FET devices through the control over the TMD film thickness [22].

In this work, we explore the high optical absorbance of multilayer TMDs and demonstrate the strong light-matter coupling between the cavity photons and neutral excitons in multilayer WSe₂ placed in a tunable, planar optical resonator. Multiple works have already demonstrated the strong coupling regime for excitons in TMD monolayers incorporated into various types of planar optical cavities [23]: dielectric [24], tunable [25, 26], metallic [27], semiconductor–metallic [28], but all of them were entirely focused on direct-bandgap ML flakes or MLs separated by thin hexagonal boron nitride (hBN) flakes [29].

The strong light-matter coupling conditions in multilayer TMDs have been recently achieved in different systems with plasmonic cavities of ultra-small volume [30, 31] and in open plasmonic cavities formed by periodic arrays of metallic nanoparticles [32]. In that case, however, the resonant electric field is polarized perpendicularly to the flakes' plane and nearly perpendicularly to the excitons' dipole moment which is mostly in-plane oriented [33]. Here we report on the observation of the strong coupling regime between photons confined in a planar cavity, where the electric field is polarized along the main axis of the excitons' dipole moment, with neutral excitons in ML as well as few-layer-thick WSe₂ flakes. Starting from the bilayer WSe₂ the bandgap becomes indirect, but the absorption at direct excitonic resonance is efficient enough to allow for creation of strongly coupled light-matter states. The exciton-photon coupling strength reaches even higher values for multilayers than for the ML due to increased thickness of the TMD material. Our findings are well reproduced by calculations done within the framework of a transfer matrix method, where the parameters of the excitonic resonances in WSe₂ are determined based on the analysis of reflectance spectra of the flakes deposited directly onto the bottom distributed Bragg reflector (DBR).

* Barbara.Pietka@fuw.edu.pl

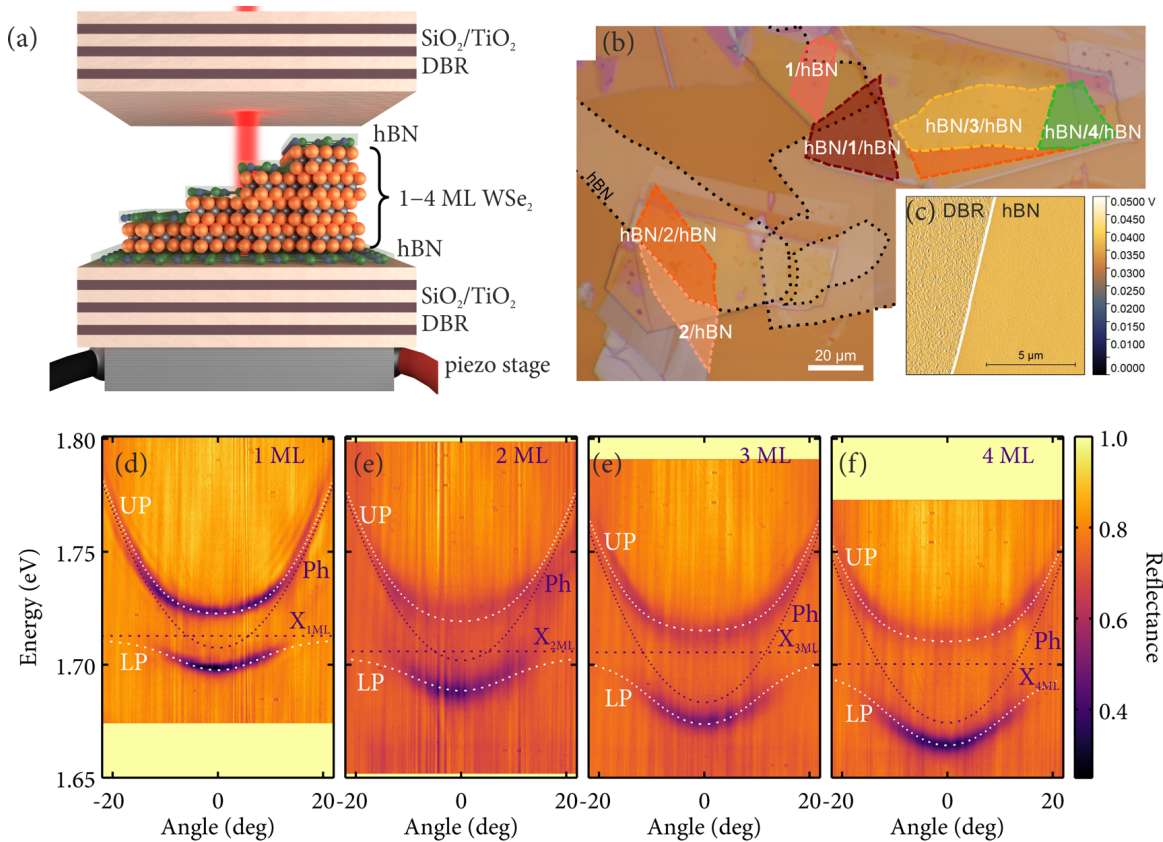


FIG. 1. (a) Scheme of a tunable cavity with few-layer flakes of WSe_2 encapsulated in hBN. (b) Microscopic image of investigated WSe_2/hBN and $\text{hBN}/\text{WSe}_2/\text{hBN}$ heterostructures deposited onto a distributed Bragg reflector (DBR). (c) Amplitude image obtained with the help of an atomic force microscope operated in the tapping mode, revealing the difference in surface roughness between the DBR and hBN. (d-f) Angle-resolved reflectance spectra of $\text{hBN}/\text{WSe}_2/\text{hBN}$ heterostructures with 1 ML- to 4 ML-thick WSe_2 flakes shown in (b) embedded in a dielectric cavity. The white dashed lines mark fitted upper and lower polariton dispersion relations given by a coupled oscillators model with the energies of the uncoupled excitonic and photonic modes drawn with the purple dashed lines.

II. RESULTS

We investigated 1 ML- to 4 ML-thick WSe_2 flakes embedded in an open, tunable dielectric cavity schematically shown in Fig. 1(a). The cavity consists of two dielectric distributed Bragg reflectors (DBRs), each made of 5 pairs of $\text{SiO}_2/\text{TiO}_2$ layers with the maximum reflectance at 723 nm (1.715 eV), chosen specifically to match the energy of the A exciton in monolayer WSe_2 encapsulated in hBN [34]. The mirrors were grown on a transparent fused silica substrate to provide optical access also from the back side.

WSe_2 flakes were mechanically exfoliated from commercially available, nominally undoped bulk crystals. Selected flakes of 1 to 4 ML thickness were then transferred onto approx. 183 nm thick (see Fig. S1 Supplementary Materials) hBN flakes previously deposited on top of the bottom DBR. The thickness of the bottom hBN flakes was chosen to obtain the local maximum of the electric field standing wave inside the final full cavity at

the position of the WSe_2 flakes to assure the efficient exciton-photon coupling conditions (see Supplementary Materials for details). The hBN capping layer covering the WSe_2 flakes was much thinner, approx. 10 nm. Fig. 1(b) presents an optical microscope image of the investigated WSe_2 flakes. The hBN encapsulation allows to significantly reduce the inhomogeneous broadening of spectral lines, leading to linewidths that approach the radiative decay limit [35, 36].

The influence of the encapsulation is still under investigation [37], but hBN provides isolation of the electrostatic disorder at the SiO_2 interfaces and acts also as an atomically flat substrate for the flakes. A comparison of surface roughness of the DBR and the hBN flake deposited on that DBR, measured by atomic force microscopy, is shown in the inset of Fig. 1(c).

The full cavity, presented in Fig. 1(a), is formed by covering the structure discussed above with another DBR. We performed angle-resolved reflectance measurements at 5 K revealing the strong coupling regime between the cavity photons and the excitons in all 1- to 4 ML-thick

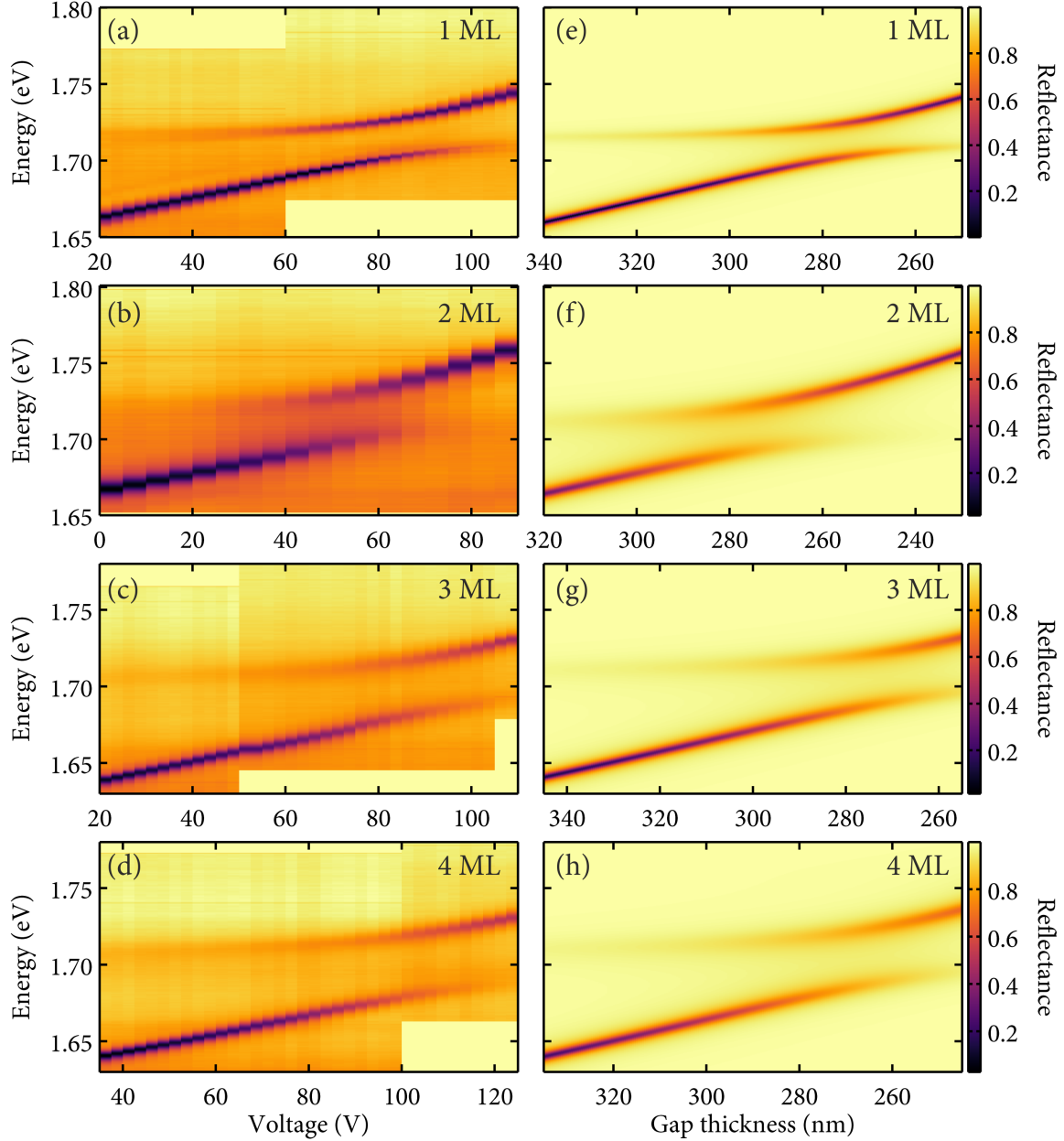


FIG. 2. Left column: maps showing experimental reflectance spectra for different voltages applied to a piezoelement tuning the cavity width, measured at 5 K and normal incidence on hBN-encapsulated: (a) 1 ML, (b) 2 ML, (c) 3 ML, (d) 4 ML WSe₂ flakes. Right column: transfer matrix method simulations of the experimental data shown in the left column, performed for: (e) 1 ML, (f) 2 ML, (g) 3 ML, (h) 4 ML as a function of distance between the DBR mirrors.

WSe₂ flakes, as presented in Fig. 1(d-f). In an angle-resolved experiment, the cavity photon energy (Ph) depends quadratically on the in-plane wavevector, which is proportional to the emission angle. The strong coupling regime of the cavity mode with the exciton resonances in thin WSe₂ layers (X_i) manifests itself by the appearance of two anticrossing lower and upper polariton branches (LP and UP), with dispersion relations well described by

a two coupled oscillators model, as demonstrated with dashed white curves in Fig. 1(d-f).

The energy of photons confined in the cavity was tuned in a continuous way by smoothly changing the distance between the mirrors [38]. Experimentally, it was realized by placing one of the mirrors on a piezoelectric stage and applying to it an external bias. Reflectance spectra at normal incidence for variable electrical bias applied to the

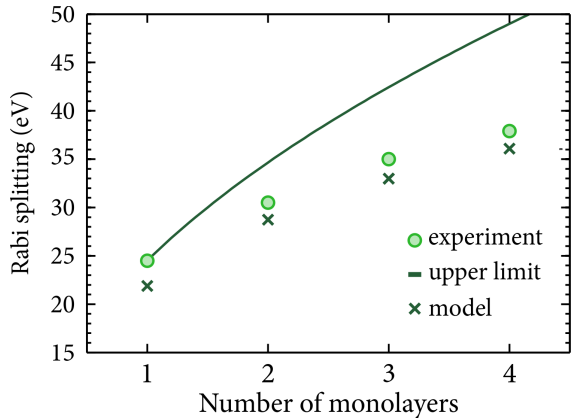


FIG. 3. Coupling strength between the photonic cavity mode and the excitonic resonance in multilayer WSe₂. The upper limit shows the highest possible coupling strength that could be achieved for a structure consisting of multiples of WSe₂ monolayers. Marked with crosses are modelled values of the multilayer coupling strength obtained from calculations based on a transfer matrix method.

piezoelectric chip taken at the position of a specific WSe₂ flake are presented in Fig. 2. Upon applying the voltage, the distance between the DBRs decreases, which results in the increase of the cavity photon energy. When the mode approaches the energy of the excitonic resonance in a given WSe₂ flake, a clear anticrossing behaviour can be observed. The minimal energy separation between the modes is equal to the coupling strength Ω , also referred to as the vacuum field Rabi splitting. The observed coupling strength increases with the number of WSe₂ layers, as shown in Fig. 3.

The coupling strength between a photonic mode of a planar cavity incorporating an optically active layer with an excitonic resonances can be in general well approximated by [39, 40]:

$$\Omega = 2\sqrt{\frac{fd}{Ln_c^2}}, \quad (1)$$

where L is the effective cavity length, n_c is the cavity refractive index and f is proportional to the exciton oscillator strength in a layer of thickness d . The coupling strength given by eq. (1) can provide the upper limit for the Rabi splitting: one can expect an increase of the coupling strength proportional to the square root of the active layer thickness, as plotted with a solid line in Fig. 3. In our experiment we observed a slower increase of the coupling strength with the number of WSe₂ layers as compared to that given by the upper limit described above and derived for the monolayer case. Such behaviour can be caused by two factors: change of the exciton resonance width or decrease of the exciton oscillator strength in multilayer WSe₂ with respect to the monolayer.

To evaluate the influence of both these factors we performed reflectance contrast (RC) and photoluminescence

(PL) measurements without the top DBR. RC spectra taken on each WSe₂ flake are presented in Fig. 4. The spectra are dominated by a pronounced dip around 1.71 eV, corresponding to the absorption of a neutral free exciton formed at the K^\pm valleys, i.e. the so-called A exciton [9]. For a monolayer, this excitonic transition is also observable in the PL spectrum, which is dominated by a broad band attributed to the so-called localised excitons [41–44]. With the increase of WSe₂ layer thickness, the energy of the excitonic resonance observed in the RC slightly decreases and broadens, with the most significant difference occurring between the monolayer and the bilayer. For WSe₂ thicker than the monolayer, as the bandgap changes from direct to indirect, the transitions related to the A excitons can no longer be observed in the PL spectra. For 2 MLs, the emission occurring at around 1.53 eV is related to the indirect bandgap transitions [41].

The high optical quality of hBN encapsulated flakes allow to observe in RC the first excited exciton states, i.e. $2s$ [45–48], shown in the insets in Fig. 4(a). Their energy separation from the main absorption line significantly decreases with the number of layers due to the expected decrease of the neutral exciton’s binding energy [45].

To extract both the exciton oscillator strength and exciton resonance linewidth, the RC spectra were fitted using a transfer matrix method. The RC signal was calculated based on simulated reflectance of the DBR and the DBR with a corresponding WSe₂ layer encapsulated in hBN. The exciton resonance was introduced as a dielectric function of the WSe₂ layer given by a Lorentz model in the form provided in [49]:

$$\varepsilon_{\text{WSe}_2}(E) = \varepsilon_0 - \sum_i \frac{f_i}{E_i^2 - E^2 - i\gamma_i E}, \quad (2)$$

where i describes the excitonic ground state and the first excited $2s$ state. The optical response of the system is also directly dependent on the thicknesses inserted into the transfer matrix model, which makes f_i defined in eq. (2) a measure of the transition strength per unit thickness of a given WSe₂ layer. Depending on the number of constituent monolayers, WSe₂ the thickness of a given WSe₂ flake was taken as a multiple of the single layer thickness equal to 0.65 nm [50]. The dielectric constant away from the resonances was taken as $\varepsilon_0 = 16$ [49].

The transfer matrix model curves were directly fitted to the experimental RC spectra with f_i , E_i and γ_i treated as fitting parameters. The results are presented with solid color lines in Fig. 4. All fitting parameters are also summarised in Tab. I. Fig. 4(b) shows the energies of excitonic resonances in hBN encapsulated WSe₂ flakes of different thicknesses. The ground state energy is almost independent of the layer thickness, whereas the energy of the excited exciton state significantly decreases. For the monolayer, the $2s$ state is 130 meV above the ground state and for the tetra-layer this energy difference decreases to 61 meV. Also the exciton’s ground state oscillator strength [see Fig. 4(c)] slightly decreases with the

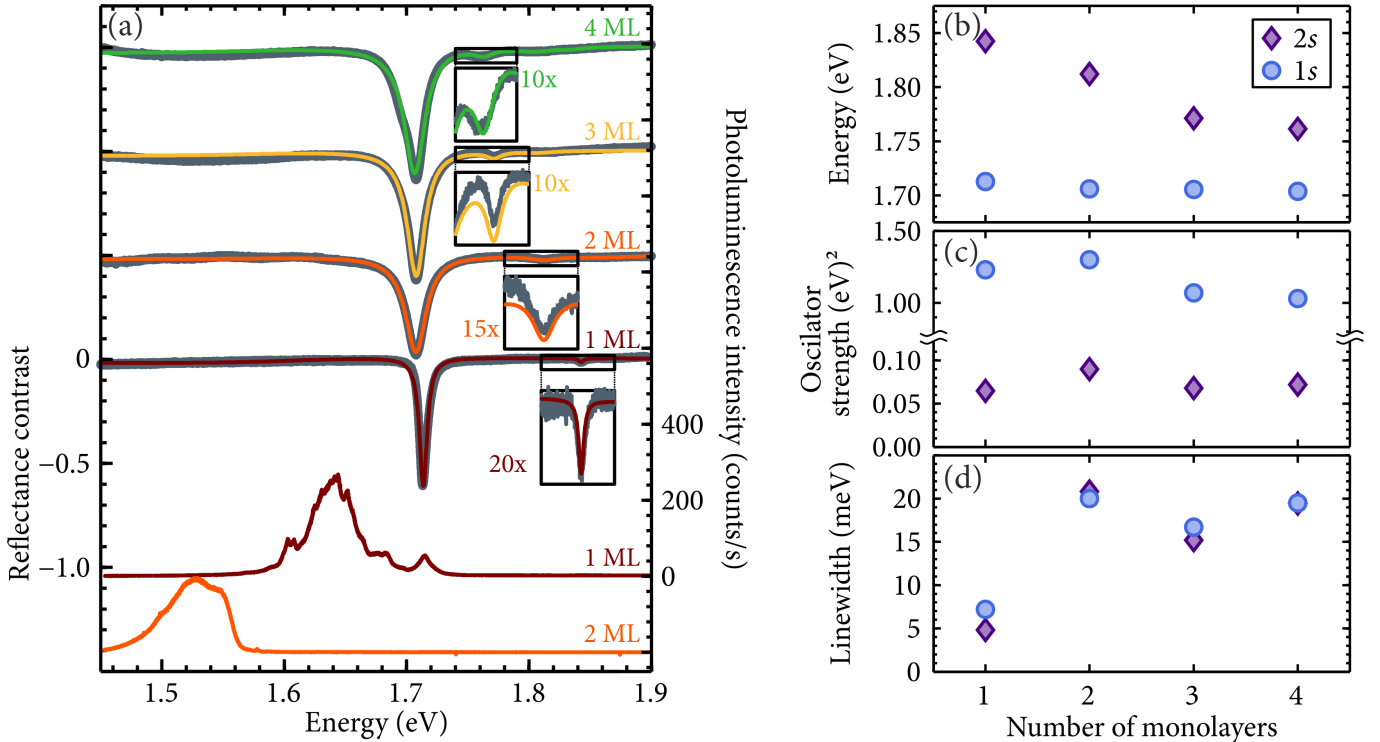


FIG. 4. (a) Reflectance contrast (RC) and photoluminescence (PL) spectra of hBN encapsulated WSe₂ multilayers measured without the top DBR at 5K. Experimental RC spectra are marked with grey lines, whereas the color curves represent the results of fitting the data with a transfer-matrix-based model. Shown in the right column are the fitting parameters of the ground and first excited exciton resonances in multilayer WSe₂: the energy position (b), the oscillator strength (c) and the linewidth (d).

TABLE I. RC fitting parameters for hBN encapsulated WSe₂ layers deposited on a DBR and a comparison of the modelled exciton-photon coupling strength in a dielectric cavity (abbrev. model) to the values obtained experimentally (abbrev. exp.).

	E_{1s} (eV)	f_{1s} (eV ²)	γ_{1s} (meV)	$\Omega_{1s}^{\text{model}}$ (meV)	Ω_{1s}^{exp} (meV)	E_{2s} (eV)	f_{2s} (eV ²)	γ_{2s} (meV)
1 ML	1.7128	1.23	7.2	21.9	24.5	1.8426	0.065	4.8
2 ML	1.7059	1.30	20.0	28.7	30.5	1.8122	0.090	20.8
3 ML	1.7055	1.07	16.7	33.0	35.0	1.7713	0.068	15.2
4 ML	1.7036	1.03	19.5	36.9	36.1	1.7632	0.072	19.4

number of layers. For the excited exciton states the oscillator strength is 19 to 14 times smaller than for the corresponding ground state with no evident dependence on the number of layers.

It is worth to mention that due to low oscillator strength of the excited $2s$ exciton state in our samples, we do not observe a strong coupling regime at this transition, as shown in Fig. S9. Such a coupling with excited exciton states has recently become of interest due to large optical nonlinearities one can probe in this type of systems [51, 52]. In our structures, the $2s$ exciton-polariton is expected to occur with $\Omega = 3.2$ meV (see Fig. S10), which is much lower than the linewidth of the $2s$ resonance as shown in Fig. 4(c).

The exciton resonance linewidth determines the optical quality of the layers and is usually affected by homogeneous and inhomogeneous contributions. For both the ground state and the excited $2s$ state, the spectrally

narrowest transition occurs in the monolayer. For the bilayer, the linewidth increases over two times, and then is almost constant for 3- and 4ML-thick layers. Starting from the 3ML thick flake, the excitonic resonances reveal a double structure. The appearance of such a fine structure (an increase of the linewidth or a presence of two partially overlapping resonances) can be explained in terms of hybridisation occurring predominantly in the valence band of thicker TMD layers (>1 ML), due to different symmetries of the conduction and valence band orbitals (see Ref. [12] for details). The analogous effect has already been observed for multilayers of WS₂ deposited on Si/SiO₂ substrate [12] and for mono- and few-layer MoS₂ encapsulated in hBN [53, 54].

The exciton properties obtained from the RC measurements of the WSe₂ layers deposited on the DBRs were used to simulate their behaviour inside a full cavity structure, as presented in Fig. 2(e-h). We used the transfer

matrix method to simulate the reflectance at normal incidence from a whole structure consisting of two DBRs and a WSe₂ flake encapsulated in hBN for variable spacing between the mirrors. The calculations well reproduce the experimental reflectance maps from the left column of Fig. 2. The exciton–photon coupling strength was extracted from the reflectance maps as the minimum energy distance between the two polaritonic branches, and then included in Fig. 3. As can be seen, the simulations slightly underestimate the coupling strength, but properly reconstruct the trend of increasing coupling strength with the thickness of WSe₂ layer.

III. SUMMARY

In summary, we have demonstrated a strong coupling regime between photons in a planar optical cavity and excitons in multilayer WSe₂. We have investigated flakes encapsulated in hBN as well as unprotected ones. The strong coupling is observed regardless of the crossover from direct to indirect bandgap accompanying the transition from the monolayer to N -layer thickness. Despite the decrease of the excitons’ oscillator strength per layer thickness at the $K\pm$ points of the Brillouin zone in few-layer WSe₂, the observed coupling strength increases with the thickness of an active WSe₂ layer which proves that multilayers can be well adopted to operate in the strong light-matter coupling regime with substantial absorption at the polariton modes. By changing the number of WSe₂ layers and controlling the distance between the Bragg mirrors we were able to tune the energies of the system eigenstates – the exciton-polaritons. Recently, it has been demonstrated that exciton-polaritons in TMDs can be coupled to the emission of a semiconductor quantum well [28, 55], or organic dye [26] forming hybrid TMDs-semiconductor-light states. Although indirect transitions analyzed in this paper would decrease the efficiency of such emission, the TMD multilayers should definitely be considered as potential building blocks for future engineering of hybrid TMDs eigenstates.

METHODS

Optical measurements

All optical measurements were performed on samples placed in a cryostat at the temperature of 5 K. PL sig-

nal was excited nonresonantly with a 514.5 nm (2.41 eV) laser beam. The excitation power, measured before the entrance of a microscope objective, was equal to 100 μ W and concentrated in approx. 1 μ m spot. For reflectance and RC measurements a broadband halogen lamp was used with a spot size of approx. 5 μ m.

Investigations of the cavity structures were performed with angular resolution, achieved by imaging the Fourier space of a high numerical aperture ($NA = 0.55$) microscope objective. Data shown in Fig. 2 corresponds to reflectance at normal incidence extracted from the angle-resolved spectra.

Demonstration of strong light-matter coupling regime and formation of the exciton-polariton modes in 1 to 6 ML thick WSe₂ flakes, which have not been encapsulated in hBN, can be found in supplementary material.

ACKNOWLEDGEMENTS

The authors thank Artur Slobodeniuk for helpful discussions. This work has been supported by the Ministry of Higher Education Republic of Poland budget for education via the research projects "Diamantowy Grant" 0109/DIA/2015/44 and 0005/DIA/2016/45; by the National Science Centre: grants 2013/10/M/ST3/00791, 2018/31/B/ST3/02111 and 2018/31/N/ST3/03046; by the EU Graphene Flagship project (ID: 785219), and the ATOMOPTO project (TEAM programme of the Foundation for Polish Science co-financed by the EU within the ERD Fund). B.P. acknowledges Ambassade de France en Pologne for the research stay project. K.W. and T.T. acknowledge support from the Elemental Strategy Initiative conducted by the MEXT, Japan and the CREST (JPMJCR15F3), JST.

-
- [1] A. K. Geim and I. V. Grigorieva, “Van der Waals heterostructures,” *Nature* **499**, 419 (2013).
 [2] Kin Fai Mak and Jie Shan, “Photonics and optoelectronics of 2D semiconductor transition metal dichalcogenides,” *Nat. Photonics* **10**, 216–226 (2016).

- [3] L. Britnell, R. M. Ribeiro, A. Eckmann, R. Jalil, B. D. Belle, A. Mishchenko, Y.-J. Kim, R. V. Gorbachev, T. Georgiou, S. V. Morozov, A. N. Grigorenko, A. K. Geim, C. Casiraghi, A. H. C. Neto, and K. S. Novoselov, “Strong light-matter interactions in heterostructures of

- atomically thin films,” *Science* **340**, 1311–1314 (2013).
- [4] F. H. L. Koppens, T. Mueller, Ph. Avouris, A. C. Ferrari, M. S. Vitiello, and M. Polini, “Photodetectors based on graphene, other two-dimensional materials and hybrid systems,” *Nat. Nanotechnol.* **9**, 780–793 (2014).
- [5] Jongtae Ahn, Pyo Jin Jeon, Syed Raza Ali Raza, Atiye Pezeshki, Sung-Wook Min, Do Kyung Hwang, and Seongil Im, “Transition metal dichalcogenide heterojunction PN diode toward ultimate photovoltaic benefits,” *2D Mater.* **3**, 045011 (2016).
- [6] Jiang Pu and Taishi Takenobu, “Monolayer transition metal dichalcogenides as light sources,” *Adv. Mater.* **30**, 1707627 (2018).
- [7] J. Binder, J. Howarth, F. Withers, M. R. Molas, T. Taniguchi, K. Watanabe, C. Faugeras, A. Wymolek, M. Danovich, V. I. Fal’ko, A. K. Geim, K. S. Novoselov, M. Potemski, and A. Kozikov, “Upconverted electroluminescence via Auger scattering of interlayer excitons in van der Waals heterostructures,” *Nat. Commun.* **10**, 2335 (2019).
- [8] Gang Wang, Alexey Chernikov, Mikhail M. Glazov, Tony F. Heinz, Xavier Marie, Thierry Amand, and Bernhard Urbaszek, “Colloquium: Excitons in atomically thin transition metal dichalcogenides,” *Rev. Mod. Phys.* **90**, 021001 (2018).
- [9] Maciej Koperski, Maciej R. Molas, Ashish Arora, Karol Nogajewski, Artur O. Slobodeniuk, Clement Faugeras, and Marek Potemski, “Optical properties of atomically thin transition metal dichalcogenides: Observations and puzzles,” *Nanophotonics* **6**, 1289–1308 (2017).
- [10] Andrea Splendiani, Liang Sun, Yuanbo Zhang, Tianshu Li, Jonghwan Kim, Chi-Yung Chim, Giulia Galli, and Feng Wang, “Emerging photoluminescence in monolayer MoS₂,” *Nano Lett.* **10**, 1271–1275 (2010).
- [11] Kin Fai Mak, Changgu Lee, James Hone, Jie Shan, and Tony F. Heinz, “Atomically thin MoS₂: A new direct-gap semiconductor,” *Phys. Rev. Lett.* **105**, 136805 (2010).
- [12] Maciej R. Molas, Karol Nogajewski, Artur O. Slobodeniuk, Johannes Binder, Miroslav Bartos, and Marek Potemski, “The optical response of monolayer, few-layer and bulk tungsten disulfide,” *Nanoscale* **9**, 13128 (2017).
- [13] Sanfeng Wu, Sonia Buckley, John R. Schaibley, Liefeng Feng, Jiaqiang Yan, David G. Mandrus, Fariba Hatami, Wang Yao, Jelena Vučković, Arka Majumdar, and Xiaodong Xu, “Monolayer semiconductor nanocavity lasers with ultralow thresholds,” *Nature* **520**, 69–72 (2015).
- [14] Yu Ye, Zi Jing Wong, Xiufang Lu, Xingjie Ni, Hanyu Zhu, Xianhui Chen, Yuan Wang, and Xiang Zhang, “Monolayer excitonic laser,” *Nat. Photonics* **9**, 733–737 (2015).
- [15] Yongzhuo Li, Jianxing Zhang, Dandan Huang, Hao Sun, Fan Fan, Jiabin Feng, Zhen Wang, and C. Z. Ning, “Room-temperature continuous-wave lasing from monolayer molybdenum ditelluride integrated with a silicon nanobeam cavity,” *Nat. Nanotechnol.* **12**, 987–992 (2017).
- [16] D. N. Basov, M. M. Fogler, and F. J. García de Abajo, “Polaritons in van der Waals materials,” *Science* **354**, aag1992 (2016).
- [17] Christian Schneider, Mikhail M. Glazov, Tobias Korn, Sven Höfling, and Bernhard Urbaszek, “Two-dimensional semiconductors in the regime of strong light-matter coupling,” *Nat. Commun.* **9**, 2695 (2018).
- [18] Andor Kormányos, Guido Burkard, Martin Gmitra, Jaroslav Fabian, Viktor Zólyomi, Neil D Drummond, and Vladimir Fal’ko, “k-p theory for two-dimensional transition metal dichalcogenide semiconductors,” *2D Mater.* **2**, 022001 (2015).
- [19] Gui-Bin Liu, Di Xiao, Yugui Yao, Xiaodong Xu, and Wang Yao, “Electronic structures and theoretical modelling of two-dimensional group-vib transition metal dichalcogenides,” *Chem. Soc. Rev.* **44**, 2643–2663 (2015).
- [20] Jessica Lindlau, Malte Selig, Andre Neumann, Léo Colombier, Jonathan Förste, Victor Funk, Michael Förg, Jonghwan Kim, Gunnar Berghäuser, Takashi Taniguchi, Kenji Watanabe, Feng Wang, Ermin Malic, and Alexander Högele, “The role of momentum-dark excitons in the elementary optical response of bilayer WSe₂,” *Nat. Commun.* **9**, 2586 (2018).
- [21] Yuanzheng Li, Jia Shi, Heyu Chen, Rui Wang, Yang Mi, Cen Zhang, Wenna Du, Shuai Zhang, Zheng Liu, Qing Zhang, Xiaohui Qiu, Haiyang Xu, Weizhen Liu, Yichun Liu, and Xinfeng Liu, “The Auger process in multilayer WSe₂ crystals,” *Nanoscale* **10**, 17585–17592 (2018).
- [22] Pushpa Raj Pudasaini, Akinola Oyedele, Cheng Zhang, Michael G. Stanford, Nicholas Cross, Anthony T. Wong, Anna N. Hoffman, Kai Xiao, Gerd Duscher, David G. Mandrus, Thomas Z. Ward, and Philip D. Rack, “High-performance multilayer WSe₂ field-effect transistors with carrier type control,” *Nano Research* **11**, 722–730 (2018).
- [23] N Lundt, A Maryński, E Cherotchenko, A Pant, X Fan, S Tongay, G Şek, A V Kavokin, S Höfling, and C Schneider, “Monolayered MoSe₂: a candidate for room temperature polaritonics,” *2D Mater.* **4**, 015006 (2016).
- [24] Xiaoze Liu, Tal Galfsky, Zheng Sun, Fengnian Xia, Erh-Chen Lin, Yi-Hsien Lee, Stéphane Kéna-Cohen, and Vinod M. Menon, “Strong light-matter coupling in two-dimensional atomic crystals,” *Nat. Photonics* **9**, 30 (2014).
- [25] S. Dufferwiel, T. P. Lyons, D. D. Solnyshkov, A. A. P. Trichet, A. Catanzaro, F. Withers, G. Malpuech, J. M. Smith, K. S. Novoselov, M. S. Skolnick, D. N. Krizhanovskii, and A. I. Tartakovskii, “Valley coherent exciton-polaritons in a monolayer semiconductor,” *Nat. Commun.* **9**, 4797 (2018).
- [26] Lucas C. Flatten, David M. Coles, Zhengyu He, David G. Lidzey, Robert A. Taylor, Jamie H. Warner, and Jason M. Smith, “Electrically tunable organic-inorganic hybrid polaritons with monolayer WS₂,” *Nat. Commun.* **8**, 14097 (2017).
- [27] Zheng Sun, Jie Gu, Areg Ghazaryan, Zav Shotan, Christopher R. Consideine, Michael Dollar, Biswanath Chakraborty, Xiaoze Liu, Pouyan Ghaemi, Stéphane Kéna-Cohen, and Vinod M. Menon, “Optical control of room-temperature valley polaritons,” *Nat. Photonics* **11**, 491 (2017).
- [28] Max Waldherr, Nils Lundt, Martin Klaas, Simon Betzold, Matthias Wurdack, Vasilij Baumann, Eliezer Estrecho, Anton Nalitov, Evgenia Cherotchenko, Hui Cai, Elena A. Ostrovskaya, Alexey V. Kavokin, Sefaattin Tongay, Sebastian Klembt, Sven Höfling, and Christian Schneider, “Observation of bosonic condensation in a hybrid monolayer MoSe₂-GaAs microcavity,” *Nat. Commun.* **9**, 3286 (2018).
- [29] S. Dufferwiel, S. Schwarz, F. Withers, A. A. P. Trichet, F. Li, M. Sich, O. Del Pozo-Zamudio, C. Clark, A. Nalitov, D. D. Solnyshkov, G. Malpuech, K. S. Novoselov,

- J. M. Smith, M. S. Skolnick, D. N. Krizhanovskii, and A. I. Tartakovskii, "Exciton-polaritons in van der Waals heterostructures embedded in tunable microcavities," *Nat. Commun.* **6**, 8579 (2015).
- [30] Marie-Elena Kleemann, Rohit Chikkaraddy, Evgeny M. Alexeev, Dean Kos, Cloudy Carnegie, Will Deacon, Alex Casalis de Pury, Christoph Große, Bart de Nijs, Jan Mertens, Alexander I. Tartakovskii, and Jeremy J. Baumberg, "Strong-coupling of WSe₂ in ultra-compact plasmonic nanocavities at room temperature," *Nat. Commun.* **8**, 1296 (2017).
- [31] Michael Stührenberg, Battulga Munkhbat, Denis G. Baranov, Jorge Cuadra, Andrew B. Yankovich, Tomasz J. Antosiewicz, Eva Olsson, and Timur Shegai, "Strong light-matter coupling between plasmons in individual gold bi-pyramids and excitons in mono- and multilayer WSe₂," *Nano Lett.* **18**, 5938–5945 (2018).
- [32] Shaojun Wang, Quynh Le-Van, Fabio Vaianella, Bjorn Maes, Simone Eizagirre Barker, Rasmus H. Godiksen, Alberto G. Curto, and Jaime Gomez Rivas, "Limits to strong coupling of excitons in multilayer WS₂ with collective plasmonic resonances," *ACS Photonics* **6**, 286–293 (2019).
- [33] Jon A. Schuller, Sinan Karaveli, Theanne Schiros, Keliang He, Shyuan Yang, Ioannis Kymissis, Jie Shan, and Rashid Zia, "Orientation of luminescent excitons in layered nanomaterials," *Nat. Nanotechnol.* **8**, 271 (2013).
- [34] M. Manca, M. M. Glazov, C. Robert, F. Cadiz, T. Taniguchi, K. Watanabe, E. Courtade, T. Amand, P. Renucci, X. Marie, G. Wang, and B. Urbaszek, "Enabling valley selective exciton scattering in monolayer WSe₂ through upconversion," *Nat. Commun.* **8**, 14927 (2017).
- [35] F. Cadiz, E. Courtade, C. Robert, G. Wang, Y. Shen, H. Cai, T. Taniguchi, K. Watanabe, H. Carrere, D. Lagarde, M. Manca, T. Amand, P. Renucci, S. Tongay, X. Marie, and B. Urbaszek, "Excitonic linewidth approaching the homogeneous limit in MoS₂-based van der Waals heterostructures," *Phys. Rev. X* **7**, 021026 (2017).
- [36] Obafunso A Ajayi, Jenny V Ardelean, Gabriella D Shepard, Jue Wang, Abhinandan Antony, Takeshi Taniguchi, Kenji Watanabe, Tony F Heinz, Stefan Strauf, X-Y Zhu, and James C Hone, "Approaching the intrinsic photoluminescence linewidth in transition metal dichalcogenide monolayers," *2D Mater.* **4**, 031011 (2017).
- [37] H. H. Fang, B. Han, C. Robert, M. A. Semina, D. Lagarde, E. Courtade, T. Taniguchi, K. Watanabe, T. Amand, and B. Urbaszek, "Control of the Exciton Radiative Lifetime in van der Waals Heterostructures," arXiv e-prints, arXiv:1902.00670 (2019), arXiv:1902.00670 [cond-mat.mes-hall].
- [38] Mateusz Król, Katarzyna Lekenta, Rafał Mirek, Karolina Lempicka, Daniel Stephan, Karol Nogajewski, Maciej R. Molas, Adam Babiński, Marek Potemski, Jacek Szczytko, and Barbara Piętka, "Valley polarization of exciton-polaritons in monolayer WSe₂ in a tunable microcavity," *Nanoscale* **11**, 9574–9579 (2019).
- [39] L. C. Flatten, Z. He, D. M. Coles, A. A. P. Trichet, A. W. Powell, R. A. Taylor, J. H. Warner, and J. M. Smith, "Room-temperature exciton-polaritons with two-dimensional WS₂," *Sci. Rep.* **6**, 33134 (2016).
- [40] V. Savona, L.C. Andreani, P. Schwendimann, and A. Quattropani, "Quantum well excitons in semiconductor microcavities: Unified treatment of weak and strong coupling regimes," *Solid State Commun.* **93**, 733–739 (1995).
- [41] Ashish Arora, Maciej Koperski, Karol Nogajewski, Jacques Marcus, Clément Faugeras, and Marek Potemski, "Excitonic resonances in thin films of WSe₂: from monolayer to bulk material," *Nanoscale* **7**, 10421–10429 (2015).
- [42] T. Smoleński, M. Goryca, M. Koperski, C. Faugeras, T. Kazimierczuk, A. Bogucki, K. Nogajewski, P. Kosacki, and M. Potemski, "Tuning valley polarization in a WSe₂ monolayer with a tiny magnetic field," *Phys. Rev. X* **6**, 021024 (2016).
- [43] T Smoleński, T Kazimierczuk, M Goryca, M R Molas, K Nogajewski, C Faugeras, M Potemski, and P Kosacki, "Magnetic field induced polarization enhancement in monolayers of tungsten dichalcogenides: effects of temperature," *2D Mater.* **5**, 015023 (2017).
- [44] Maciej Koperski, Maciej R Molas, Ashish Arora, Karol Nogajewski, Miroslav Bartos, Jan Wyzula, Diana Vavclavkova, Piotr Kossacki, and Marek Potemski, "Orbital, spin and valley contributions to zeeman splitting of excitonic resonances in MoSe₂, WSe₂ and WS₂ monolayers," *2D Mater.* **6**, 015001 (2018).
- [45] Alexey Chernikov, Timothy C. Berkelbach, Heather M. Hill, Albert Rigosi, Yilei Li, Ozgur Burak Aslan, David R. Reichman, Mark S. Hybertsen, and Tony F. Heinz, "Exciton binding energy and nonhydrogenic rydberg series in monolayer WS₂," *Phys. Rev. Lett.* **113**, 076802 (2014).
- [46] Keliang He, Nardeep Kumar, Liang Zhao, Zefang Wang, Kin Fai Mak, Hui Zhao, and Jie Shan, "Tightly bound excitons in monolayer WSe₂," *Phys. Rev. Lett.* **113**, 026803 (2014).
- [47] Shao-Yu Chen, Thomas Goldstein, Jiayue Tong, Takashi Taniguchi, Kenji Watanabe, and Jun Yan, "Superior valley polarization and coherence of 2s excitons in monolayer WSe₂," *Phys. Rev. Lett.* **120**, 046402 (2018).
- [48] M. R. Molas, A. O. Slobodeniuk, K. Nogajewski, M. Bartos, Ł. Bala, A. Babiński, K. Watanabe, T. Taniguchi, C. Faugeras, and M. Potemski, "Energy spectrum of two-dimensional excitons in a nonuniform dielectric medium," *Phys. Rev. Lett.* **123**, 136801 (2019).
- [49] Yilei Li, Alexey Chernikov, Xian Zhang, Albert Rigosi, Heather M. Hill, Arend M. van der Zande, Daniel A. Chenet, En-Min Shih, James Hone, and Tony F. Heinz, "Measurement of the optical dielectric function of monolayer transition-metal dichalcogenides: MoS₂, MoSe₂, WS₂, and WSe₂," *Phys. Rev. B* **90**, 205422 (2014).
- [50] B. Radisavljevic, A. Radenovic, J. Brivio, V. Giacometti, and A. Kis, "Single-layer MoS₂ transistors," *Nat. Nanotechnol.* **6**, 147 (2011).
- [51] Jie Gu, Lutz Waldecker, Daniel Rhodes, Alexandra Boehmke, Archana Raja, Rian Koots, James C. Hone, Tony F. Heinz, and Vinod M. Menon, "Nonlinear interaction of Rydberg exciton-polaritons in two-dimensional WSe₂," *Conference on Lasers and Electro-Optics*, FW3M.5 (2019).
- [52] Valentin Walther, Robert Johne, and Thomas Pohl, "Giant optical nonlinearities from rydberg excitons in semiconductor microcavities," *Nature Commun.* **9** (2018), 10.1038/s41467-018-03742-7.
- [53] A O Slobodeniuk, Ł Bala, M Koperski, M R Molas, P Kossacki, K Nogajewski, M Bartos, K Watanabe, T Taniguchi, C Faugeras, and M Potemski, "Fine

- structure of k-excitons in multilayers of transition metal dichalcogenides,” *2D Mater.* **6**, 025026 (2019).
- [54] Iann C. Gerber, Emmanuel Courtade, Shivangi Shree, Cedric Robert, Takashi Taniguchi, Kenji Watanabe, Andrea Balocchi, Pierre Renucci, Delphine Lagarde, Xavier Marie, and Bernhard Urbaszek, “Interlayer excitons in bilayer MoS₂ with strong oscillator strength up to room temperature,” *Phys. Rev. B* **99**, 035443 (2019).
- [55] Matthias Wurdack, Nils Lundt, Martin Klaas, Vasilij Baumann, Alexey V. Kavokin, Sven Höfling, and Christian Schneider, “Observation of hybrid Tamm-plasmon exciton- polaritons with GaAs quantum wells and a MoSe₂ monolayer,” *Nat. Commun.* **8**, 259 (2017).

Supplementary information for Exciton-polaritons in multilayer WSe₂ in a planar microcavity

M. Król,¹ K. Rechcińska,¹ K. Nogajewski,¹ M. Grzeszczyk,¹ K. Łempicka,¹ R. Mirek,¹ S. Piotrowska,¹
K. Watanabe,² T. Taniguchi,² M. R. Molas,¹ M. Potemski,^{1,3} J. Szczytko,¹ and B. Piętka^{1,*}

¹*Institute of Experimental Physics, Faculty of Physics,
University of Warsaw, ul. Pasteura 5, PL-02-093 Warsaw, Poland*

²*National Institute for Materials Science, Tsukuba, Ibaraki, 305-0044, Japan*

³*Laboratoire National des Champs Magnétiques Intenses,
CNRS-UGA-UPS-INSA-EMFL, Grenoble, France*

I. hBN CHARACTERISATION

To ensure the most effective light–matter coupling the WSe₂ layer should be positioned at the antinode of the standing wave of the electromagnetic field inside the cavity. For cavity without hBN such requirement can be fulfilled when DBRs are ending with lower refractive index material: SiO₂. Using the same DBRs for encapsulated WSe₂, lower hBN layer should have optical thickness of $\lambda_0/2$. For the excitonic transition in monolayer WSe₂ at approx. 710 nm and hBN refractive index of 2.1 [1], this corresponds to approx. 170 nm.

The exfoliated hBN flakes with comparative thickness were transferred to the DBRs. Images of the transferred hBN with the corresponding height profiles measured by AFM are presented in Fig. S1.

II. EMPTY CAVITY

Reflectance from a tunable cavity without active WSe₂ flakes is presented in Fig. S2. Measurements were taken from the position of 183 nm thick hBN layer. All of the measurements of the cavity structures were angle-resolved. Fig. S2(a) shows reflectance maps obtained at two different electric biases applied to the piezoelectric chip, which was used to tune the distance between the mirror. Full tunability range for voltages 0–150 V is shown in Fig. S2(a), which presents reflectance at normal incidence. Data for incidence perpendicular to the cavity plane was selected from the angle-resolved maps. The cavity mode resonance energy shifts over 150 meV linearly with voltage.

In Fig. S2(c) experimental position and linewidth of the cavity mode is compared with transfer matrix simulations. The air-gap thickness taken for simulations were extracted from the experimental energy position of the cavity mode. Reflectance deep linewidth, at the order of 5 meV, is almost constant up to 110 V, and slightly increases for thinner cavity. This behaviour is consistent with transfer matrix simulations marked by blue line in Fig. S2(c), but the calculated linewidths are slightly lower

than is observed experimentally. Such broadening of experimental results can be explained when the mirrors forming the cavity are not perfectly parallel. Measuring reflectance with a 5 μm Gaussian spot we average over such area. This averaging can be taken into account in transfer matrix simulations with assumption, that the distance between the mirrors doesn't have a finite value, but rather is a random variable. Calculations performed for the intermirror distance described by a normal distribution with a small dispersion σ equal to 1 nm, shows better agreement between linewidth observed in the experiment and the model [purple line in Fig. S2(c)].

Fig. S2(d)] presents reflectance spectra given by such modified for broadening model for different values of the dispersion of the normal distribution.

III. WSe₂ FLAKES WITHOUT hBN ENCAPSULATION

As a reference we prepared another sample with WSe₂ flakes without hBN encapsulation. Those 1 to 6 ML thick flakes were deposited directly onto a surface of a identical DBR, as described in the main text. Performed reflectance contrast (RC) and photoluminescence (PL) measurements of the on top mirror are presented in Fig. S4(a).

For the WSe₂ monolayer the RC spectrum measured in the vicinity of the optical bandgap, consists of a single narrow deep at 1.753 eV, corresponding to the absorption of a neutral free exciton (so-called A exciton) [2]. For the bilayer, the absorption transition is observed at lower energies and significantly broadens. Starting from the 3 ML thick flakes, the related resonances reveal a doubled structure. Appearance of such fine structure can be explained by the hybridisation of the valence and conduction bands in TMD layers (>1 ML), as has already been observed for multilayers of WS₂ deposited on Si/SiO₂ substrate [3] and of MoS₂ encapsulated in hBN [4, 5]

For monolayer, the PL spectrum is dominated by a broad band attributed to the so-called localised excitons [6–8]. The inset in Fig. S4(a) shows a weaker peak at higher energies, which is associated with the emission of free neutral A excitons. Its energy coincides with the energy of the corresponding A resonance apparent in the RC spectrum. The emission energy and

* Barbara.Pietka@fuw.edu.pl

intensity decrease significantly for thicker WSe₂ flakes, as the bandgap change from direct one for the ML to indirect one in multilayers. For the 2 and 3MLs, the observed emission occurring correspondingly at around 1.55 eV and 1.42 eV is related to the indirect band gap [6].

IV. FLAKES DEPOSITED ON hBN WITHOUT CAPPING LAYER

We investigated also two additional monolayer and a bilayer WSe₂ flakes isolated from the DBR by hBN, but without the thin covering hBN flake. Photoluminescence and reflectance contrast spectra without the top mirror are shown in Fig. S7 for monolayer and in Fig. S8 for bilayer. Optical properties of those flakes, like linewidth and emission intensity, are similar to the fully encapsulated WSe₂. The excitonic transition energies are in between dielectric-screened encapsulated flakes and the deposited directly on the DBR. 2s excited exciton tran-

sitions are not observed in the reflectance measurement.

V. COUPLING WITH 2s EXCITON STATE

Tuning the cavity mode to the 2s exciton resonance energy visible on reflectance contrast spectra for encapsulated monolayer flake does not reveal any sign of coupling due to low value of oscillator strength of this transition. For the cavity mode energy crossing the 2s exciton resonance energy no sign of anticrossing or mode linewidth broadening is observed, as shown in Fig. S9. No sign of coupling can be seen also at angle resolved spectra shown in Fig. S9(a,b).

Such observation is consistent with the transfer matrix simulations. Fig. S10(a) shows calculated reflectance spectra for zero detuning between the cavity mode and a 2s exciton state for different values of oscillator strength. For the value determined by the fitting to the reflectance contrast measurement, simulated reflectance spectra can be well described by a sum of two Lorentz functions, but with the distance between them lower than their widths.

-
- [1] S.-Y. Lee, T.-Y. Jeong, S. Jung, and K.-J. Yee, *Phys. Status Solidi B*, 1800417 (2018).
 - [2] M. Koperski, M. R. Molas, A. Arora, K. Nogajewski, A. O. Slobodeniuk, C. Faugeras, and M. Potemski, *Nanophotonics* **6**, 1289 (2017).
 - [3] M. R. Molas, K. Nogajewski, A. O. Slobodeniuk, J. Binder, M. Bartos, and M. Potemski, *Nanoscale* **9**, 13128 (2017).
 - [4] A. O. Slobodeniuk, Ł. Bala, M. Koperski, M. R. Molas, P. Kossacki, K. Nogajewski, M. Bartos, K. Watanabe, T. Taniguchi, C. Faugeras, and M. Potemski, *2D Mater.* **6**, 025026 (2019).
 - [5] I. C. Gerber, E. Courtade, S. Shree, C. Robert, T. Taniguchi, K. Watanabe, A. Balocchi, P. Renucci, D. Lagarde, X. Marie, and B. Urbaszek, *Phys. Rev. B* **99**, 035443 (2019).
 - [6] A. Arora, M. Koperski, K. Nogajewski, J. Marcus, C. Faugeras, and M. Potemski, *Nanoscale* **7**, 10421 (2015).
 - [7] T. Smoleński, M. Goryca, M. Koperski, C. Faugeras, T. Kazimierzczuk, A. Bogucki, K. Nogajewski, P. Kossacki, and M. Potemski, *Phys. Rev. X* **6**, 021024 (2016).
 - [8] M. Koperski, M. R. Molas, A. Arora, K. Nogajewski, M. Bartos, J. Wyzula, D. Vaclavkova, P. Kossacki, and M. Potemski, *2D Mater.* **6**, 015001 (2018).

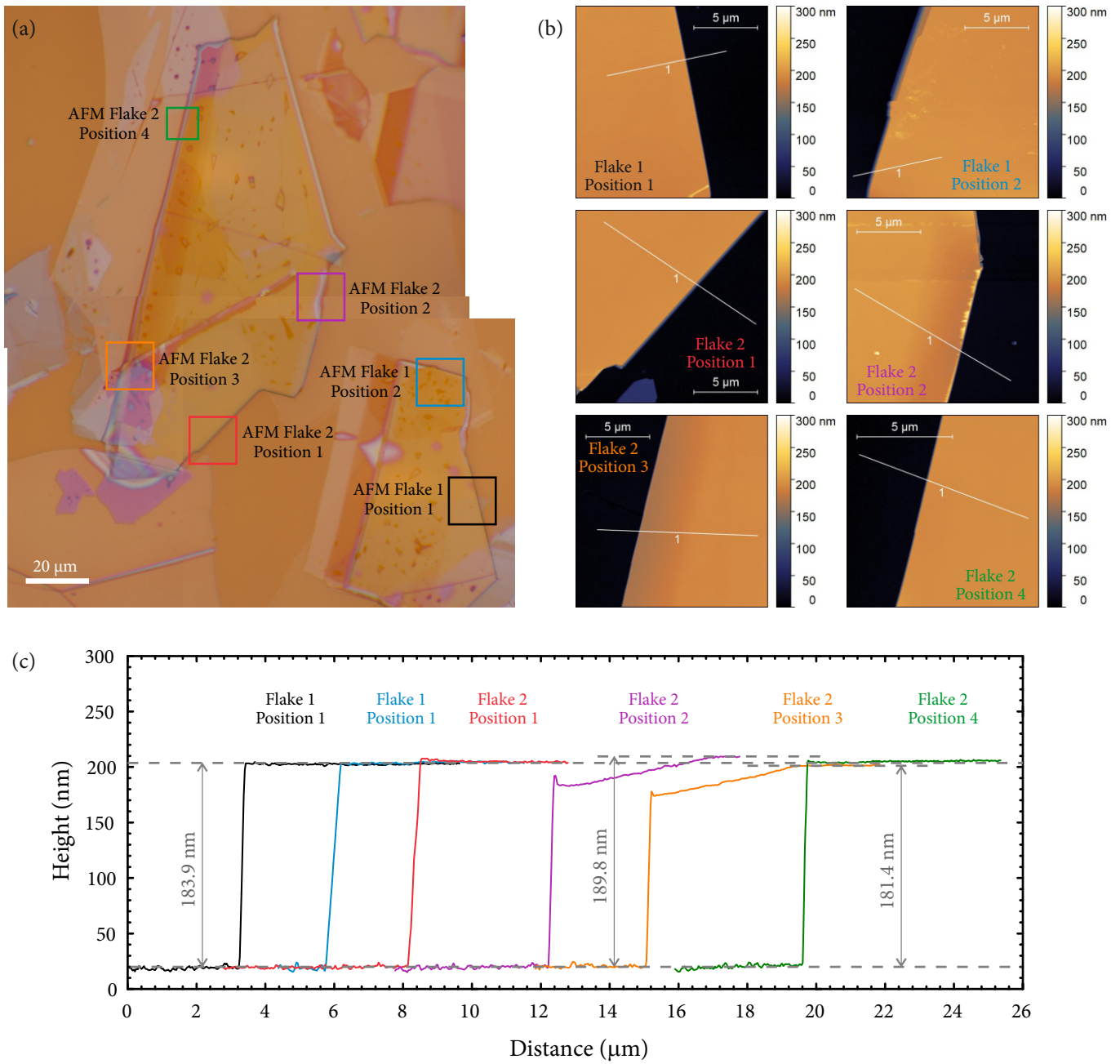


FIG. S1. Characterization of hBN layers. (a) Microscopic image of DBR surface with deposited exfoliated hBN. Marked regions were investigated using AFM and are presented in (b). (c) Height profiles along straight lines marked in (b).

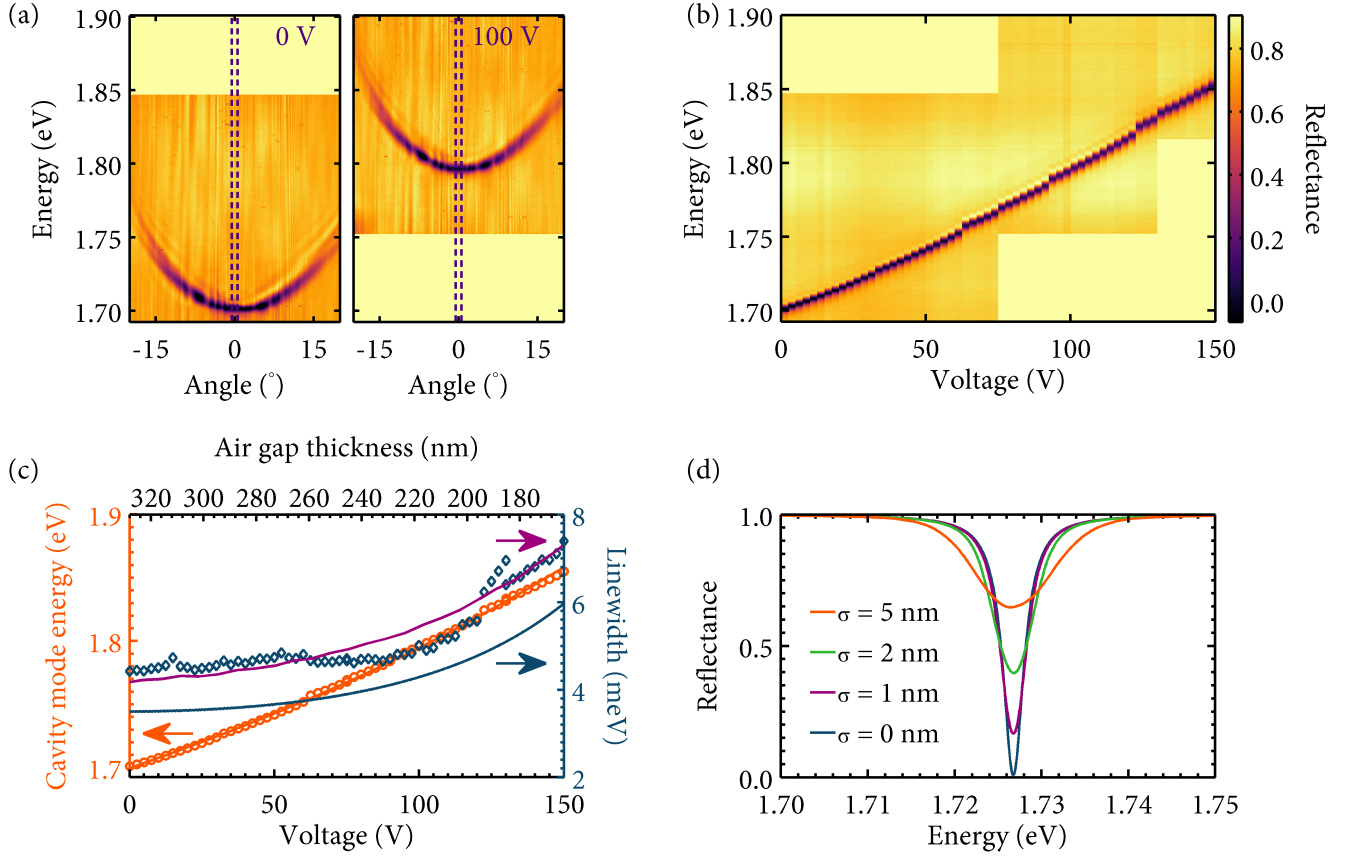


FIG. S2. Tunable cavity with with 183 nm thick hBN layer. (a) Angle-resolved reflectance spectra at two different voltages applied to the piezoelectric actuator. (b) Tuability of the cavity at normal incidence [range between the dashed lines in (a)]. (c) Experimental values of cavity mode energy and reflection deep linewidth change with bias applied to the piezoelectric chip (points) compared with transfer matrix simulations for decreasing air gap thickness (lines). Blue line shows linewidth for a perfectly parallel mirrors. Purple line marks simulation with assumption that the distance between the mirror is a random variable described by normal distribution with a dispersion $\sigma = 1$ nm. (d) Simulations of normal incidence reflectance from the cavity where the distace between the mirrors is given by normal distribution with mean value of 300 and given dispersion σ .

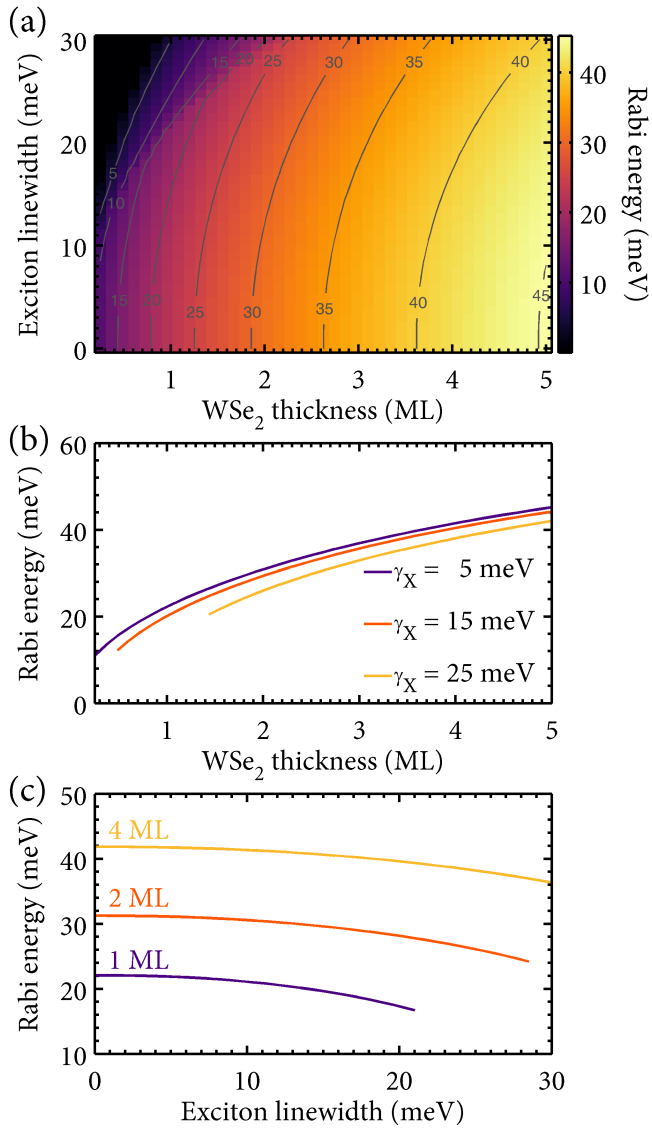


FIG. S3. Transfer matrix simulations for WSe₂ layer with $f = 1.23$ and encapsulated in hBN. (a) Rabi energy dependence on (b) WSe₂ layer thickness (c) exciton resonance linewidth.

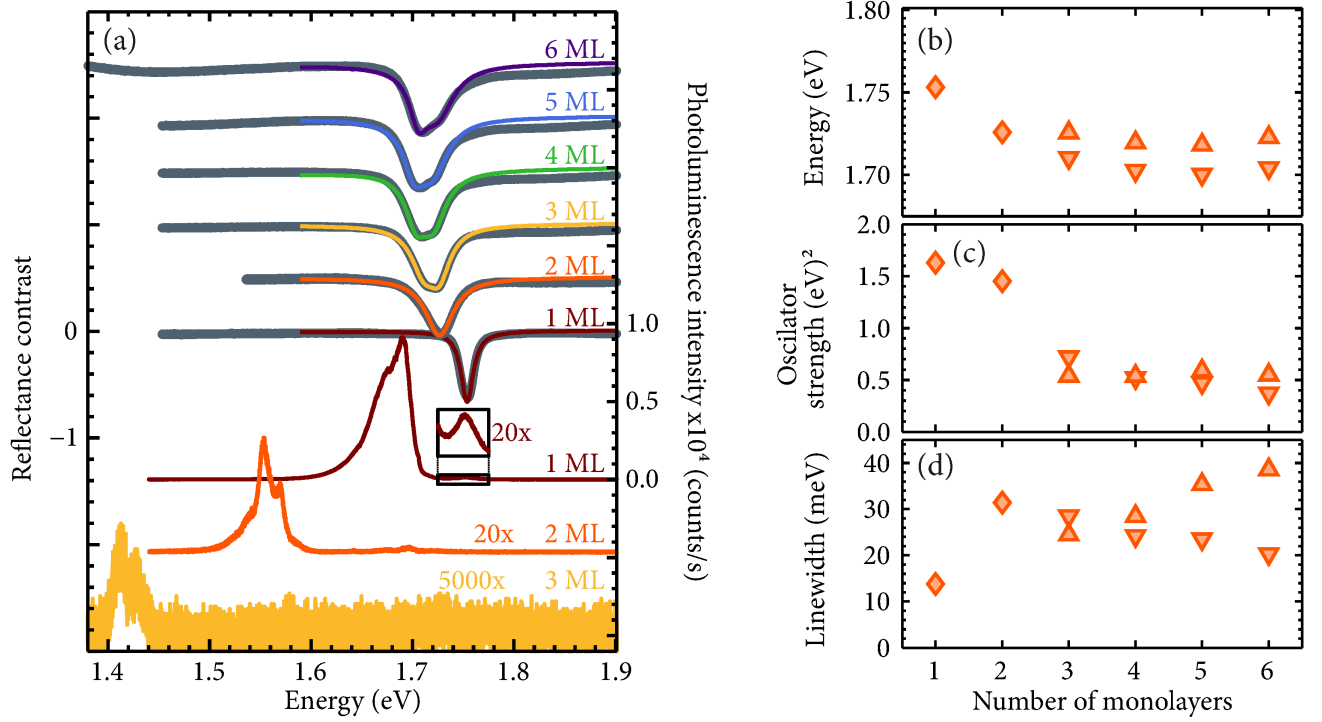


FIG. S4. (a) Reflectance contrast (RC) and photoluminescence (PL) spectra of WSe₂ multilayers deposited on top of a DBR measured at 5 K. Experimental RC spectra are marked with gray lines, whereas colour lines represent the fitted transfer matrix model. Fitting parameters of ground and first excited exciton resonances in multilayer WSe₂: (b) energy positions, (c) oscillator strength and (d) linewidth. Δ mark the fine structure components of higher energy and ∇ of the lower one.

TABLE I. RC fitting parameters for WSe₂ deposited on the DBR with modeled exciton-photon coupling strength in dielectric cavity (abbrev. model) compared with the values obtained experimentally (abbrev. exp).

	E_{1s} (eV)	f_{1s} (eV ²)	γ_{1s} (meV)	$\Omega_{1s}^{\text{model}}$ (meV)	Ω_{1s}^{exp} (meV)
1 ML	1.7532	1.63	13.8	19.4	23.9
2 ML	1.7258	1.45	31.4	20.8	23.2
3 ML	1.7103	0.72	28.5	29.1	30.2
	1.7257	0.54	24.5		
4 ML	1.7026	0.52	24.2	31.3	37.5
	1.7196	0.54	28.5		
5 ML	1.7002	0.47	23.5	33.6	36.8
	1.7182	0.59	35.4		
6 ML	1.7041	0.37	20.3	33.2	40.7
	1.7228	0.55	38.6		

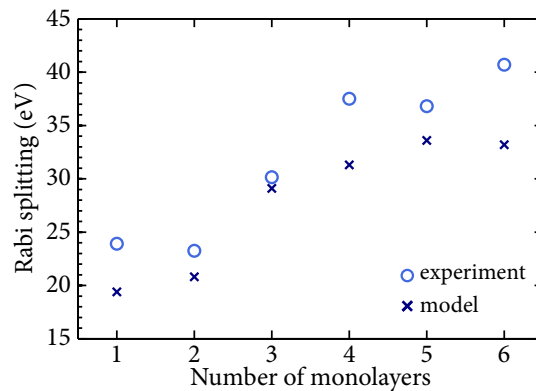


FIG. S5. Experimental coupling strength of multilayer WSe₂ flakes. Modelled values of coupling strength based on reflectance spectra calculated with transfer matrix method are marked with crosses.

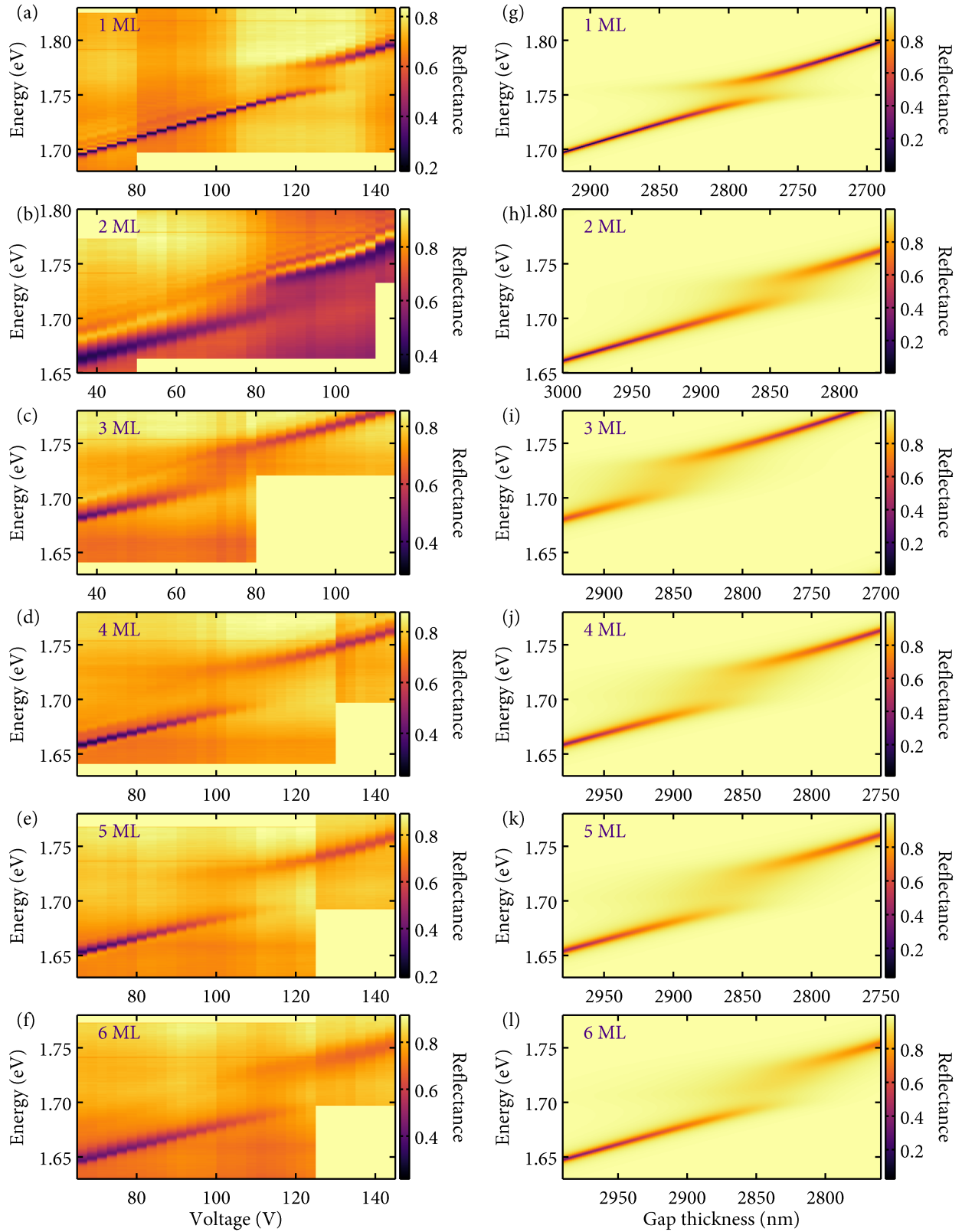


FIG. S6. WSe_2 few-layer flakes in tunable cavity. Reflectance map for normal incidence for tuning the cavity with voltage applied to the piezoelement with: (a) 1 ML, (b) 2 ML, (c) 3 ML, (d) 4 ML, (e) 5 ML and (f) 6 ML WSe_2 flakes without encapsulation. All of the measurements were performed at 5 K. Transfer matrix method simulations for variable distance between the DBR mirrors: (g) 1 ML, (h) 2 ML, (i) 3 ML, (j) 4 ML, (k) 5 ML, (l) 6 ML.

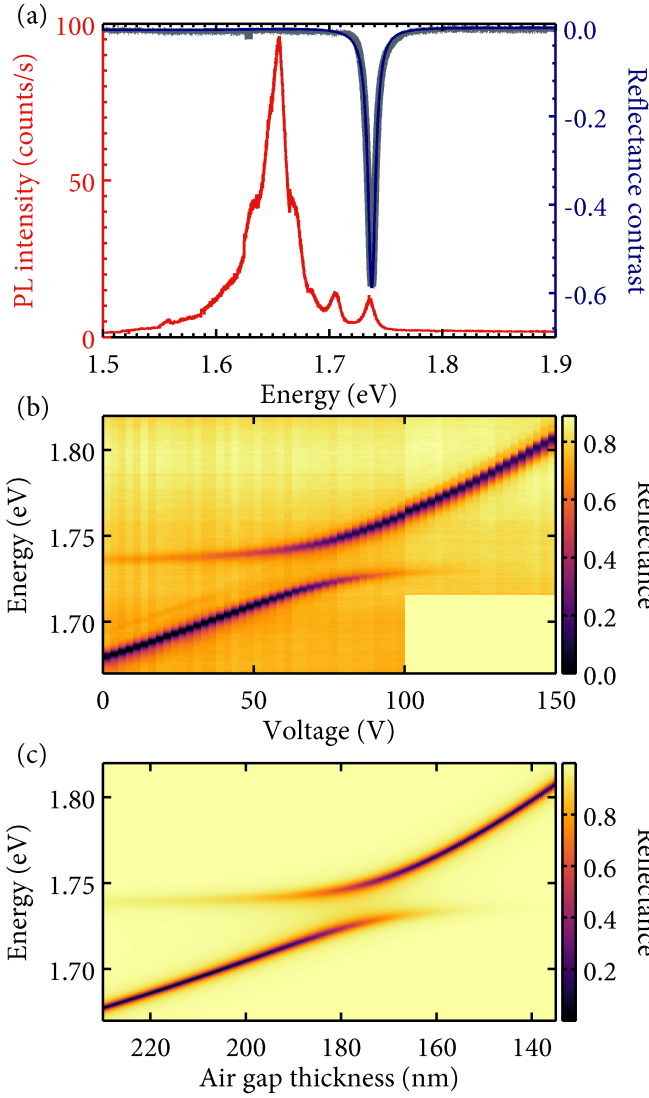


FIG. S7. WSe₂ monolayer deposited on hBN. (a) Photoluminescence (red) and reflectance contrast spectra (gray). Blue line presents fitted reflectance spectra. (b) Reflectance at normal incidence for variable cavity length. (c) Modeled reflectance map based on the fitting the blue curve in (a).

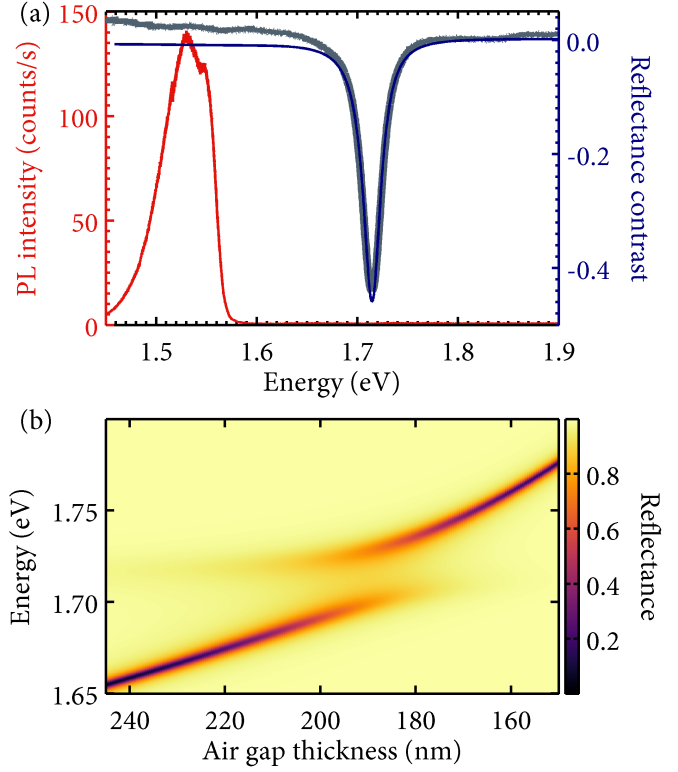


FIG. S8. WSe₂ bilayer deposited on hBN. (a) Photoluminescence (red) and reflectance contrast spectra (gray). Blue line presents fitted reflectance spectra. (b) Modeled reflectance map based on the fitting the blue curve in (a).

TABLE II. Fitting parameters for WSe₂ deposited on hBN with modelled coupling strength in dielectric cavity compared with the values obtained experimentally.

	E_{1s} (eV)	f_{1s} (eV ²)	γ_{1s} (meV)	$\Omega_{1s}^{\text{model}}$ (meV)	Ω_{1s}^{exp} (meV)
1 ML	1.7366	1.10	7.6	21.7	24.5
2 ML	1.7132	1.03	20.5	27.6	

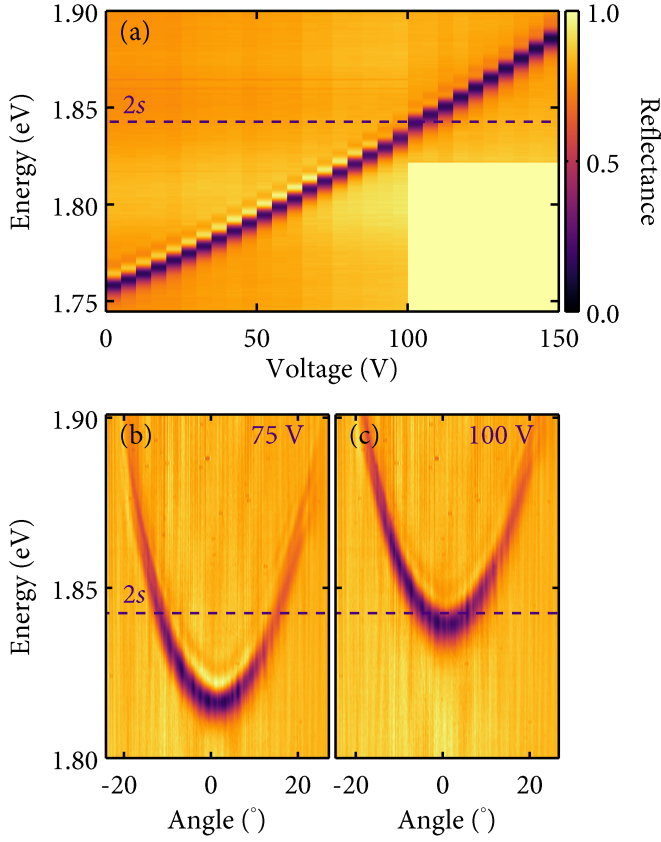


FIG. S9. Cavity resonant with $2s$ exciton transition in monolayer WSe_2 . (a) Reflectance at normal incidence with cavity mode crossing $2s$ exciton energy. Angle-resolved reflectance spectra at (b) 75 V and (c) 100 V applied to the piezoelectric chip. No sign of coupling at $2s$ state energy is visible.

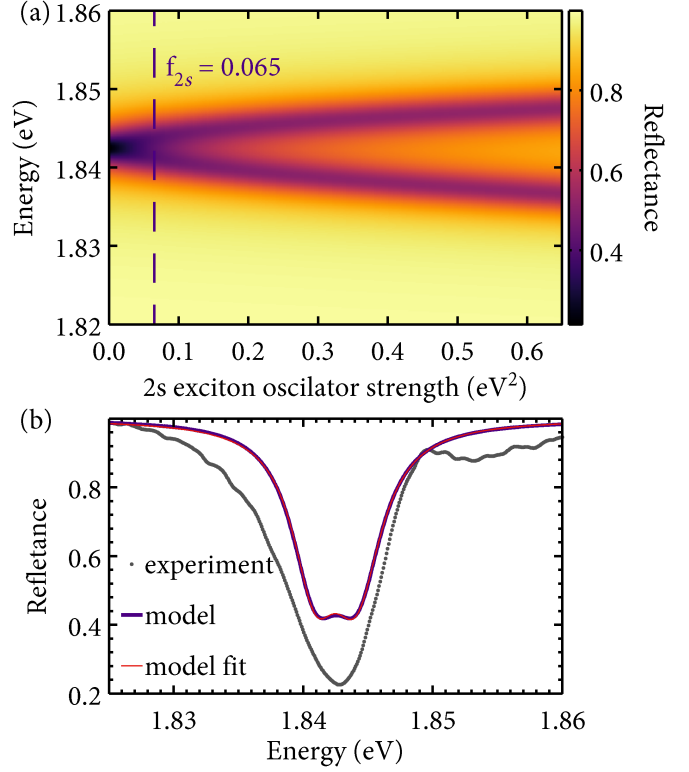


FIG. S10. Simulations for cavity resonant with $2s$ exciton transition in monolayer WSe_2 . (a) Reflectance at normal incidence calculated for various oscillator strength of $2s$ exciton f_{2s} . (b) Cross section through (a) for experimental value of f_{2s} . Sum of two Lorentz functions was fitted to the spectra giving distance between two modes of 3.2 meV, which is lower than linewidth of 4.5 meV.